High-precision temperature measurement based on weak measurement using nematic liquid crystals

Hongjing Li, Jing-Zheng Huang, Yang Yu, Yanjia Li, Chen Fang, and Guihua Zeng[a)]
State Key Laboratory of Advanced Optical Communication Systems and Networks, and Center of Quantum Information Sensing and Processing, Shanghai Jiao Tong University, Shanghai 200240, China

(Received 27 February 2018; accepted 22 May 2018; published online 4 June 2018)

High-precision temperature measurements could guarantee temperature difference control accuracy in research and industrial production. To flexibly achieve high precision and large operating temperature range is a crucial problem for temperature measurements. Here, we demonstrate a method for a high-precision temperature measurement based on a weak measurement done using nematic liquid crystals (NLCs). By performing an analysis in the frequency domain, the temperature variation of NLCs is measured using a Sagnac interferometer with appropriate preselection and postselection. In order to obtain a large operating temperature range, there is a relatively large time delay that resulted from NLCs, and an operational principle is deduced explicitly by Jones matrices. In the proposed method, the precision of $3 \times 10^{-6}\,^{\circ}\mathrm{C}$ could be achieved by a currently available spectrometer and the operating temperature range can be modulated by the thickness of NLCs. Moreover, the temperature sensitivity of 13.5 nm/°C could be realized for NLCs with 100 μm thickness, which exhibits at least three orders of magnitude larger than the value for other frequency domain analyses. *Published by AIP Publishing.*
https://doi.org/10.1063/1.5027117

Resistive thermometry is widely used in temperature measurements, but the precision is limited by drifts and resistive heating.[1] Many researchers have focused on optical methods for high-precision temperature measurements, such as displacement of optical interferometry exhibiting a precision of 2 μK at room temperature,[2] the frequency difference of fiber Bragg gratings showing an accuracy on the order of $10^{-3}\,^{\circ}\mathrm{C}$,[3] and the intensity ratio of the fluorescence spectrum with a temperature resolution of 0.2 K.[4] The high-precision temperature measurement has potential applications in the output wavelength of the distributed feedback laser,[5,6] cell culture monitoring,[7] and physical properties of the material.[8,9]

Weak measurement, which was first introduced by Aharonov, Albert, and Vaidman in 1988,[10] has attracted extensive attention and academic interest in precision metrology because it has been employed in observing some tiny physical effects, such as the spin Hall effect of light,[11] small beam deflection produced by moving mirrors,[12] velocity measurement,[13] phase shifts,[14,15] and temperature measurement.[1] Combined with appropriate preselected and postselected states, the weak measurement can lead to an amplification phenomenon and give access to experimental sensitivity beyond detector's resolution at the sacrifice of postselected probability.[11–17] Egan and Stone utilized a fluid-filled prism and interferometric weak value amplification to sense nanoradian deviations of a laser beam, which achieved a narrow 20 mK capture range with 0.2 mK precision.[1] Salazar-Serrano *et al.* enhanced the sensitivity of temperature sensors based on fiber Bragg gratings via the real part of weak value amplification,[18] which performed a spectral shift of the reflected signal of about 0.035 nm/°C.

Generally, a high precision temperature measurement and a large operating temperature range could not be achieved at the same time. How to flexibly solve this crucial problem is the key for the temperature measurement. In this letter, we investigate a method for a high-precision temperature measurement based on a weak measurement using nematic liquid crystals (NLCs) in the frequency domain. Because the time delay that resulted from NLCs for a large operating temperature range is out of restriction of the standard weak measurement, the operational principle is deduced by Jones matrices. The experimental results suggest that the highest precision of $3 \times 10^{-6}\,^{\circ}\mathrm{C}$ could be achieved by using a currently available spectrometer. The operating temperature range can be modulated by the thickness of NLCs.

A schematic illustration of the experimental setup is shown in Fig. 1. Photons emitted from a commercial LED with a measured central wavelength of $\lambda = 776$ nm and a spectral width of $\Delta\lambda = 20$ nm were collected by two lenses, and they passed through a pinhole and entered the first Glan polarizer, which preselected the polarization state. Then, the light entered a Sagnac interferometer consisting of a polarized beam splitter (PBS) and two mirrors. There were two orthogonal polarization paths divided by the PBS. The LC mixture E7 (Merck), with a wide nematic temperature range (−10 °C to 59 °C), was placed vertically in a Sagnac interferometer and considered as a temperature sensor. NLCs were sandwiched by two indium-tin oxide (ITO) glass substrates with 50 μm or 100 μm thick spacers in between. The temperature of the NLC sample was precisely controlled with an accuracy of 0.01 °C by a temperature controller (HCS302, Instec Co.). The output light passed a quarter-wave plate (QWP) rotated 45° to the fast axis and the second Glan polarizer nearly orthogonal to the first one. The light was monitored by a spectrometer with a range of 690–850 nm.

a)Electronic mail: ghzeng@sjtu.edu.cn

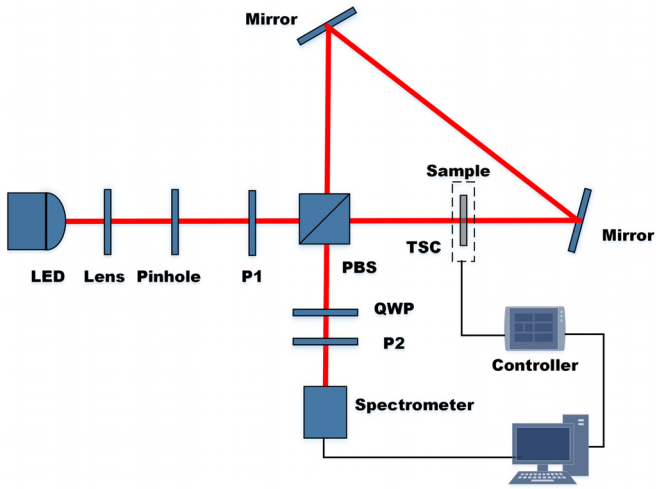

FIG. 1. Schematic diagram of the experimental setup: P, Glan polarizer; PBS, polarizing beam splitter; TSC, temperature-stabilized optical chamber; and QWP, quarter-wave plate. The NLC sample is placed in TSC with glass windows to enable the transmission of light beams.

The weak measurement includes three steps: a preselected state, a postselected state, and a weak perturbation. The preselected state and the postselected state are nearly orthogonally polarized states. In the proposed method, the weak perturbation comes from the temperature variation of NLCs. NLCs possess the largest birefringence (Δn ~0.2–0.7) from the visible to microwave band among all known materials,[19–22] which are widely used in various optoelectronic applications.[19–23] Moreover, NLCs have an exceptionally large thermo-optic coefficient (dn/dT) of $\sim 10^{-3}$/K.[20] For the uni-axial NLC sample embedded in the Sagnac interferometer, there are two different refractive indices n_e and n_o for light polarization along and perpendicular to the director axis, respectively,[21] which are strongly dependent on the temperature and the wavelength.[23] Because the refractive indices and the birefringence of NLCs are wavelength dependent, the birefringence dispersion of liquid crystals should be considered.[24] Due to the spectral bandwidth of the LED of 20 nm in the experiment, the birefringence dispersion of liquid crystals is small, which could not be considered while analyzing experimental data. The temperature dependence of the birefringence ($\Delta n = n_e - n_o$) is written as[25]

$$\Delta n(T) = (\Delta n)_0 (1 - T/T_c)^{\beta}, \tag{1}$$

where T is the temperature, $(\Delta n)_0$ is the birefringence of NLCs at $T = 0K$, β is a material constant which is not sensitive to the molecular structure of NLCs, and T_c is the clearing point of NLCs. Under the condition that $T \ll T_c$, the birefringence of NLCs decreases linearly with increasing temperature and the variation of birefringence $\Delta(\Delta n)$ is estimated by the following expression:

$$\Delta(\Delta n) = \frac{\partial(\Delta n)}{\partial T} \Delta T. \tag{2}$$

The relative phase during the birefringence variation of NLCs breaks the clockwise or counterclockwise symmetry of the Sagnac interferometer, written as

$$\varphi = \omega\tau = \frac{\omega \Delta(\Delta n) d}{c}, \tag{3}$$

where ω is the frequency of light, τ is the time delay resulting from the NLC sample, d is the cell thickness, and c is the velocity of light.

For the standard weak measurement, the time delay is extremely small satisfying $\omega_0 \tau \ll \varepsilon$, where ω_0 is the central frequency of light treated as the meter and ε denotes the postselection angle.[26] The postselected state after an evolution is deduced by the first-order approximation. In this proposed method, the large operating temperature range is considered and there will be a relatively large time delay that resulted from the NLC sample not satisfying the standard weak measurement limit. It will make a large error in the theoretical derivation of the standard weak measurement. Therefore, we deduce explicitly the operational principle of this method by using the Jones matrices.

In the experiment, we consider that the incident light is with a Gaussian distribution, which can be expressed as follows:

$$E(t) = \begin{bmatrix} E_0 \exp(-t^2\sigma^2/2) \exp(i\omega_0 t) \\ 0 \end{bmatrix}. \tag{4}$$

Based on the Fourier transform, the state can be described as

$$\begin{aligned} E(\omega) &= \int_{-\infty}^{\infty} E(t) \exp(-i\omega t) dt \\ &= \begin{bmatrix} E_0 \frac{\sqrt{2\pi}}{\sigma} \exp\left(-\frac{(\omega - \omega_0)^2}{2\sigma^2}\right) \\ 0 \end{bmatrix}. \end{aligned} \tag{5}$$

When the incident light passes through the first Glan polarizer whose azimuth angle is set to $\pi/4$, the preselected state is written as

$$E(\omega) = \begin{bmatrix} \frac{1}{2} & \frac{1}{2} \\ \frac{1}{2} & \frac{1}{2} \end{bmatrix} \begin{bmatrix} E_0 \frac{\sqrt{2\pi}}{\sigma} \exp\left(-\frac{(\omega - \omega_0)^2}{2\sigma^2}\right) \\ 0 \end{bmatrix}. \tag{6}$$

After introducing the relative phase φ that resulted from the NLC sample with temperature variation, the weak perturbation in the Sagnac interferometer is described by

$$\begin{aligned} U &= \begin{bmatrix} \exp(i\varphi) & 0 \\ 0 & \exp(-i\varphi) \end{bmatrix} \\ &= \begin{bmatrix} \exp(i\omega\tau) & 0 \\ 0 & \exp(-i\omega\tau) \end{bmatrix}. \end{aligned} \tag{7}$$

The meter state after weak perturbation is expressed as

$$E_U(\omega) = UE(\omega). \tag{8}$$

The postselection process is performed with a QWP and the second Glan polarizer with its azimuth angle at $-\pi/4+\varepsilon$, which is given by

$$C = \begin{bmatrix} \cos^2\left(-\frac{\pi}{4}+\varepsilon\right) & \cos\left(-\frac{\pi}{4}+\varepsilon\right)\sin\left(-\frac{\pi}{4}+\varepsilon\right) \\ \cos\left(-\frac{\pi}{4}+\varepsilon\right)\sin\left(-\frac{\pi}{4}+\varepsilon\right) & \sin^2\left(-\frac{\pi}{4}+\varepsilon\right) \end{bmatrix} \frac{1}{\sqrt{2}}\begin{bmatrix} 1 & -i \\ -i & 1 \end{bmatrix}. \quad (9)$$

After postselection, the state becomes

$$E_{post}(\omega) = CE_U(\omega). \quad (10)$$

The frequency probability distribution is $\mathrm{I}(\omega) = |E_{post}(\omega)|^2$, where the distribution related to spectral shift is given by

$$\mathrm{I}_p \propto \exp\left(-\frac{(\omega-\omega_0-\tau\sigma^2/\varepsilon)^2}{\sigma^2}\right). \quad (11)$$

Thus, the spectral shift $\Delta\omega$ is given by

$$\Delta\omega = \omega - \omega_0 = \frac{\sigma^2\tau}{\varepsilon}. \quad (12)$$

According to Eq. (3) and Eq. (12), the relation between the spectral shift and the temperature variation ΔT can be written as

$$\Delta\omega = \frac{\sigma^2 d}{\varepsilon c}\frac{\partial(\Delta n)}{\partial T}\Delta T. \quad (13)$$

It indicates that the spectral shift is associated with the temperature variation resulting from the NLC sample in the proposed method.

In the experiment, we slowly varied the NLC sample temperature and recorded the corresponding changes in spectral shift. Figure 2 shows the spectral shifts as a function of NLC sample temperature variation for a given postselection. In Fig. 2, the spectral shift during sample temperature variation with 100 μm thickness increases faster than that with 50 μm thickness. Based on the relation $\omega = 2\pi c/\lambda$, the shift in the wavelength is given by

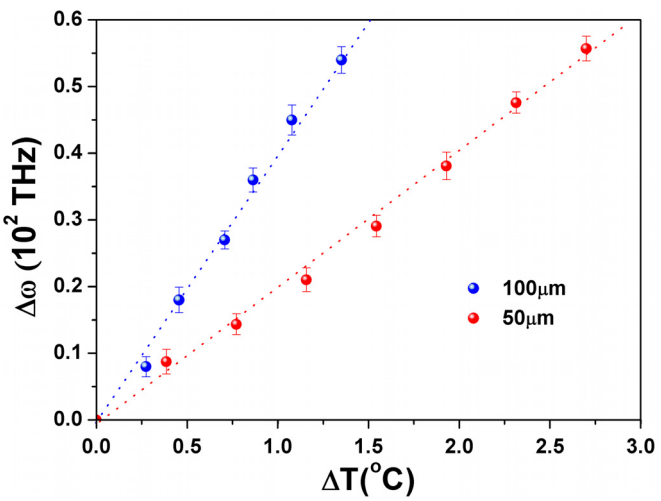

FIG. 2. Spectral shifts of light as a function of temperature variation of NLC samples with 100 and 50 μm thicknesses. The dashed lines are theoretical predictions based on Eq. (13).

$$\Delta\lambda = \frac{\Delta\omega\lambda^2}{2\pi c}. \quad (14)$$

For the NLC sample with 100 μm and 50 μm thicknesses, the temperature sensitivity could be given an estimate of 13.5 nm/°C and 6.8 nm/°C, respectively. The operating temperature range of 100 μm thickness is smaller than that of 50 μm thickness. The experimental results shown in Fig. 2, along with theoretical predictions obtained by Eq. (13), indicate that temperature sensitivity is dependent on the thickness of the NLC sample. However, the thickness of the NLC sample is limited by surface anchoring energy because the NLC director alignment quality could deform as the cell gap increases. Compared with the previous results of Ref. 18, temperature sensitivity of our proposed method is almost three orders of magnitude larger than the value for the fiber Bragg grating temperature sensor via weak value amplification. Equation (13) clearly shows that the precision of temperature measurement is associated with the resolution of the spectrometer. The currently available spectrometer has a spectral resolution of $\Delta\lambda = 0.04$ pm, which leads to a frequency resolution of $\Delta\omega = 1.2 \times 10^8$ Hz at the operating wavelength. Based on Eq. (13), we can say that the precision of temperature variation is about 3×10^{-6} °C by performing our proposed method.

The high-precision temperature measurement is attributed to the temperature sensitive material used in temperature measurement and the spectral analyses of the weak measurement in the frequency domain. Based on Eq. (13), the precision of temperature variation is associated with the thermo-optic coefficient of temperature sensitive material. NLCs possess large thermo-optic coefficients, which are sensitive to temperature variation and beneficial to improve the precision of the temperature measurement. For the weak measurement, there are two different scenarios, involving real weak value amplification and imaginary weak value amplification. Brunner and Simon pointed out that imaginary weak value amplification when combined with frequency-domain analysis outperforms real weak value amplification and interferometry by several orders of magnitude.[16] Compared with the precision of the temperature measurement shown in Ref. 1 with real weak value amplification, the measuring accuracy of our proposed method is improved by three orders of magnitude.

We plot the dependence of temperature variation on the sample thickness of NLCs calculated from Eq. (13) for the maximum spectral shift of $\Delta\omega = 0.6 \times 10^2$ THz, as shown in Fig. 3. It can be seen that the operating temperature range decreases with increasing sample thickness. The operating temperature range is sensitive to the sample thickness less than 20 μm. The change in the operating temperature range is gradually small as the thickness of the NLC sample increases. For the thinnest NLC sample ($d = 1$ μm), the

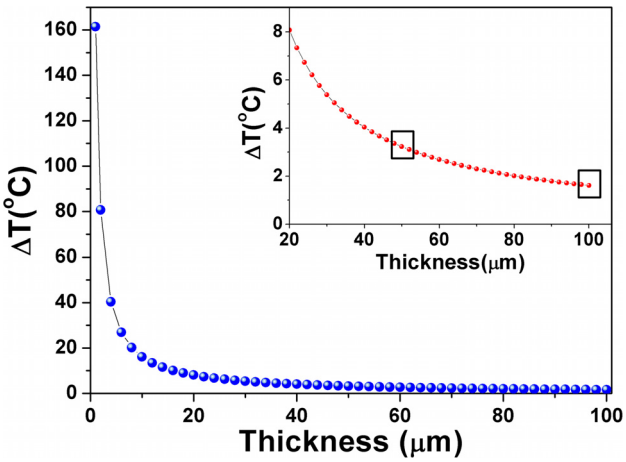

FIG. 3. Dependence of temperature variation on the sample thickness of NLCs. Inset: the temperature change with the sample thickness (20 μm < d < 100 μm). The thickness of two squares is 50 μm and 100 μm, respectively.

operating temperature range can theoretically reach up to 160 °C. In our experiment, we use the nematic phase of NLCs E7 to sense the temperature change, and the nematic temperature range of it is about 70 °C. When the sample temperature exceeds the nematic temperature range of NLCs, the sample is in the isotropic phase and the birefringence effect of NLCs disappears. As the syntheses of liquid crystals improve, the nematic temperature range of NLCs could reach up to 120 °C, such as the LC mixture ZLI-1565 (Merck). The operating temperature range of this method can be modulated by different kinds of NLCs for practical applications.

The experimental results shown in Figs. 2 and 3 indicate that the temperature sensitivity and the operating temperature range are both dependent on the thickness of the NLC sample. The fabrication technology of the NLC sample is easy, flexible, and of low-cost. The sample thickness can be modulated by the spacers between two ITO substrates. However, there is a limit to improve the precision of this temperature measurement because the thickness of the NLC sample is associated with the degree of ordering in the orientation of NLC molecules, surface roughness, and the transmittance of the sample at the operating wavelength.[20,27] Moreover, it is difficult to control accurately the thickness of the thinner NLC sample for a large operating temperature range. On the other hand, the response time of the measurement is another problem to be considered. The response time of the measurement is associated with the elastic properties of NLCs,[28–30] the processing speed, and the resolution of the spectrometer. The impact of the above-mentioned factors on the response time of the measurement is under investigation. Therefore, the precision of the temperature measurement and the operating temperature range can be modulated by the NLC sample thickness according to the practical measurement requirement.

In conclusion, we have demonstrated a method for a high-precision temperature measurement based on a weak measurement using NLCs. The precision of 3×10^{-6} °C could be achieved by using the currently available spectrometer. The operating measurement range can be modulated by the thickness of the NLC sample. The largest operating measurement range could theoretically reach up to 160 °C. The temperature sensitivity of 13.5 nm/°C is experimentally realized when the NLC sample with 100 μm thickness was embedded into the Sagnac interferometer. Taking advantage of these characteristics, the proposed method has great potential applications in high-precision temperature measurements.

This work was supported by the National Natural Science Foundation of China (Grants Nos. 61332019, 61471239, 61671287, 61631014, and 61701302), the National Key Research and Development Program (Grant No. 2016YFA0302600), and the fund of State Key Laboratory of Advanced Optical Communication Systems and Networks.

[1]P. Egan and J. A. Stone, Opt. Lett. **37**, 4991 (2012).
[2]R. David and I. W. Hunter, Sens. Actuators, A **121**, 31 (2005).
[3]Y. Lu, K. Baker, L. Chen, and X. Bao, J. Lightwave Technol. **33**, 381 (2015).
[4]C. Parigger, H. Plemmons, R. J. Litchford, and S.-M. Jeng, Opt. Lett. **23**, 76 (1998).
[5]L. Huang, P. Ma, R. Tao, C. Shi, X. Wang, and P. Zhou, Opt. Express **23**, 10506 (2015).
[6]Y. Wang, W. Yang, H. Zhou, M. Huo, and Y. Zheng, Opt. Express **21**, 18068 (2013).
[7]S. Petronis, M. Stangegaard, C. B. Christensen, and M. Dufva, Biotechniques **40**, 368 (2006).
[8]L. Lucchetti, M. Gentili, and F. Simoni, Appl. Phys. Lett. **86**, 151117 (2005).
[9]F. Catala, F. Marsa, M. Montes-Usategui, and E. Martin-Badosa, Sci. Rep. **7**, 16052 (2017).
[10]Y. Aharonov, D. Z. Albert, and L. Vaidman, Phys. Rev. Lett. **60**, 1351 (1988).
[11]O. Hosten and P. Kwiat, Science **319**, 787 (2008).
[12]P. B. Dixon, D. J. Starling, A. N. Jordan, and J. C. Howell, Phys. Rev. Lett. **102**, 173601 (2009).
[13]G. I. Viza, J. Martínez-Rincón, G. A. Howland, H. Frostig, I. Shomroni, B. Dayan, and J. C. Howell, Opt. Lett. **38**, 2949 (2013).
[14]N. Bruner and C. Simon, Phys. Rev. Lett. **105**, 010405 (2010).
[15]C.-F. Li, X.-Y. Xu, J.-S. Xu, and G.-C. Guo, Phys. Rev. A **83**, 044102 (2011).
[16]X.-Y. Xu, Y. Kedem, K. Sun, L. Vaidman, C.-F. Li, and G.-C. Guo, Phys. Rev. Lett. **111**, 033604 (2013).
[17]X. Qiu, L. Xie, X. Liu, L. Luo, Z. Li, Z. Zhang, and J. Du, Appl. Phys. Lett. **110**, 071105 (2017).
[18]L. J. Salazar-Serrano, D. Barrera, W. Amaya, S. Sales, V. Pruneri, J. Capmany, and J. P. Torres, Opt. Lett. **40**, 3962 (2015).
[19]S.-T. Wu and D.-K. Yang, *Fundamentals of Liquid Crystal Devices, Wiley Series in Display Technology* (Wiley, 2006).
[20]I. C. Khoo, Prog. Quantum Electron. **38**, 77 (2014).
[21]J. Li, S. Gauza, and S.-T. Wu, Opt. Express **12**, 2002 (2004).
[22]S. Gauza, C.-H. Wen, S.-T. Wu, N. Janarthanan, and C.-S. Hsu, Jpn. J. Appl. Phys., Part 1 **43**, 7634 (2004).
[23]J. Li, S.-T. Wu, S. Brugioni, R. Meucci, and S. Faetti, J. Appl. Phys. **97**, 073501 (2005).
[24]S.-T. Wu, Phys. Rev. A **33**, 1270 (1986).
[25]S.-T. Wu and C.-S. Wu, Phys. Rev. A **42**, 2219 (1990).
[26]Z.-H. Zhang, G. Chen, X.-Y. Xu, J.-S. Tang, W.-H. Zhang, Y.-J. Han, C.-F. Li, and G.-C. Guo, Phys. Rev. A **94**, 053843 (2016).
[27]S.-T. Wu and U. Efron, Appl. Phys. Lett. **48**, 624 (1986).
[28]E. Brasselet and S. Juodkazis, J. Nonlinear Opt. Phys. Mater. **18**, 167 (2009).
[29]E. Brasselet, T. Balciunas, N. Murazawa, S. Juodkazis, and H. Misawa, Mol. Cryst. Liq. Cryst. **512**, 143 (2009).
[30]E. Brasselet, Phys. Rev. A **82**, 063836 (2010).